YAP and ECM Stiffness: Key Drivers of Adipocyte Differentiation and Lipid Accumulation

Da-Long Dong * and Guang-Zhen Jin *

Posted Date: 8 October 2024

doi: 10.20944/preprints202410.0446.v1

Keywords: YAP ; ADSC; Hydrogel; Mechanical force; Adipose;ECM

 doi:10.20944/preprints202410.0446.v1

Article

YAP and ECM Stiffness: Key Drivers of Adipocyte Differentiation and Lipid Accumulation

Da-Long Dong [1,2] and Guang-Zhen Jin1 [1,3,*]

[1] Institute of Tissue Regeneration Engineering (ITREN), Dankook University, Cheonan, Republic of Korea
[2] Department of Nanobiomedical Science and BK21 PLUS NBM Global Research Center for Regenerative Medicine, Dankook University, Cheonan, Republic of Korea
[3] Department of Biomaterials Science, College of Dentistry, Dankook University, Cheonan, Republic of Korea
* Correspondence: gzhjin2002@dankook.ac.kr; dongdalong@dankook.ac.kr; Tel.: Tel.: +82-41-550-3082~4

Abstract: ECM stiffness significantly influences ADSC differentiation, with YAP, a major transcription factor in the Hippo signaling pathway, playing a pivotal role. This study investigates how ECM stiffness affects ADSC differentiation and its relationship with YAP signaling. Different hydrogel concentrations were used to simulate varying ECM stiffness,and their effects on ADSC differentiation were analyzed through material properties, adipocyte-specific gene expression, lipid droplet staining, YAP localization, and protein levels. Results showed that increasing hydrogel stiffness enhanced adipocyte differentiation in a gradient manner. Inhibition of YAP signaling further increased lipid droplet accumulation, suggesting ECM stiffness affects adipogenesis by modulating YAP signaling and its cytoplasmic phosphorylation. This study reveals the molecular mechanism of ECM stiffness-dependent lipid deposition, highlighting YAP's regulatory role in adipogenesis. These findings provide insights into cell differentiation regulation and have implications for tissue engineering and obesity treatment strategies.

Keywords: YAP; ADSC; hydrogel; mechanical force; Adipose; ECM

1. Introduction

The extracellular matrix (ECM) significantly influences adipocyte differentiation and plasticity, affecting both their maturation and potential for dedifferentiation [1,2]. Recent studies have revealed the complex interactions between ECM components and adipocytes, highlighting the mechanisms regulating the adipocyte differentiation process. For example, ECM proteins like fibronectin and type I collagen can substantially improve mature adipocyte conversion into DFATs with an increase in their stem cell-like properties [2]. A similar test using d-ECM autografts successfully induced adipogenic differentiation of ADSCs via the ERK1/2-PPARγ signaling pathway, which is crucial for adipocyte maturation [3,4].

Early works on mechanotransduction utilized 2D culture models in the studies on the influence of stiffness on cell migration, proliferation, malignancy, and differentiation [5–9] . These works elaborated this concept of mechanotransduction and showed that such findings do apply in vivo. However, in most cases, a 3D cultural environment better presents behavior that is relevant biologically [10,11]. A 3D microenvironment can sustain the chondrogenic phenotype [12], differentiate between normal mammary epithelial cells and breast cancer cells—where only normal cells form growth-arrested acinar structures [13], support fibrous adhesion in fibroblasts as observed in vivo [11], enhance the pluripotency of human embryonic stem cells [14], and regulate the angiogenic capacity of tumor cells [15]. Notably, recent evidence indicates that 3D mechanotransduction is fundamentally different from 2D mechanotransduction [16–19].

ECM stiffness and hydrogels regulate YAP activity: Being a major driver of mechanotransduction, YAP can alter stem cell fate through the perception of and response to

 doi:10.20944/preprints202410.0446.v1

mechanical signals provided by ECM stiffness.In 2D cultures, YAP nuclear localization changes with substrate size and stiffness, stiffer ECM facilitates YAP translocation into the nucleus, promoting cell differentiation pathways [20]. However, the 3D culture microenvironment is critical for the in vivo-like behavior and may differentially impact YAP compared to 2D systems.For example, hydrogels of tunable stiffness can drive lineage-specific differentiation of stem cells through regulating the mechanosensing ability of YAP [21].In 3D cultures, spatially directing YAP nuclear translocation via hydrogel degradation patterns further mediates ADSC differentiation [22].

YAP and its interaction with mechanical signals: A stiff ECM can activate YAP, promoting changes in glycolysis and mitochondrial dynamics, processes that are crucial for stem cell differentiation [23].In engineered hydrogels, an increase in stiffness significantly enhances YAP signaling, thereby promoting cell remodeling and differentiation processes [24]. This mechanosensing capability of YAP enables it to integrate physical signals from the ECM and influence the differentiation pathways of adipose-derived stem cells by regulating downstream gene expression [25].

We utilized 3D collagen hydrogels with adjustable matrix stiffness to replicate the in vivo microenvironment and systematically examine the impact of hydrogel matrix stiffness on ADSC differentiation. Our work searched for an explanation of how adipose stem cells perceive the surrounding microenvironment in the 3D hydrogel and favor the process of adipocyte differentiation. Material phenotype analyses, gene expression, YAP nuclear translocation, Western blotting, and adipogenesis-related fluorescence quantification were conducted to elucidate YAP's role in adipocyte differentiation regulation.

2. Materials and Methods

2.1. Cell Culture

SD rats were obtained from JSBIO, Korea, and housed at Dankook University's animal facility with ad libitum access to food and water under a 12-hour light/dark cycle.All animal experiments adhered to the ARRIVE guidelines and were approved by the Dankook University Institutional Animal Care and Use Committee, following relevant regulations. Inguinal fat tissue from 4-week-old Sprague-Dawley rats was aseptically harvested using sterile surgical scissors. The tissue was minced and digested with 0.2% collagenase type I by continuous shaking at 37°C for 30minutes. The digested mixture was filtered through a 40-micron cell strainer to eliminate undigested tissue fragments. The cells were cultured in high-glucose DMEM with 10% FBS and 1% PS. When the cell confluence reached 80%, cell cryopreservation was performed. Passage 4 (P4) cells were used for the experiments.

2.2. Hydrogel Preparation

A hydrogel matrix consisting of rat tail collagen I (Corning Incorporated Product batch number:354236) at 3.47mg/mL was used in this study.Hydrogels were prepared at concentrations of 0.5, 1 and 2 mg/mL according to the manufacturer's instructions and experimental criteria.Dilute Dulbecco's modified Eagle's medium (DMEM High Glucose LM 001-05) and collagen in the specified volume ratio. Adjust the pH to 7.2 using 1N sodium hydroxide solution. Dispense 100μL of the hydrogel mixture into silicone molds with a 0.9cm diameter. Incubate at 37°C for 20 minutes to allow gelation. After gelation, gently demold and add differentiation medium, as detailed in Supplementary (Figure S1).

2.3. Stress and Elastic Modulus Testing of Adipose Tissue and Hydrogels

We selected abdominal fat tissue from 6-week-old rats, ensuring it was harvested as intact as possible. The fat tissue was strip-shaped, becoming progressively thicker from left to right. The tissue was divided into three sections, named APT, MPT, and PPT, for testing. The same compression testing method used for the hydrogels was applied, with a maximum compression of 60% every 200 seconds.

 doi:10.20944/preprints202410.0446.v1

The cell-free hydrogels were soaked in distilled water until reaching swelling equilibrium, after which their mechanical properties were evaluated using a dynamic mechanical analyzer. The compressive modulus was measured by applying a 60% compressive strain at a strain rate of 200seconds^-1 at room temperature, utilizing the CellScale MicroTester mechanical testing instrument (CellScale, Canada). Each test group consisted of five parallel samples, and the average of the results was calculated.

$$\sigma = \frac{F}{A} \qquad E = \frac{\sigma}{\varepsilon}$$

σ: Stress in units of pascals (Pa)
F: The force applied to the material, in units of newtons (N)
A: The material's cross-sectional area, measured in square meters (m^2)
E: Young's modulus, is measured in pascals (Pa).
ϵ: strain(%)

2.4. Adipose Stem Cells Differentiate into Adipocytes in Hydrogel

We studied the adipogenic differentiation process of 15,000 ADSCs embedded in collagen hydrogels in passage 4(P4).Hydrogels were cultured in DMEM high glucose medium supplemented with 10% fetal bovine serum (FBS) and 1%(v/v) penicillin-streptomycin (100U/mL penicillin, 100 μg/mL streptomycin; Sigma Aldrich, UK). Differentiation medium included ITS1X (BD Biosciences, UK), 10nM dexamethasone (Sigma Aldrich, UK), and 283.897 μM ascorbic acid. Hydrogels were maintained at 37°C with 5%CO2 in a cell culture incubator, and the differentiation medium was refreshed every other day during the 9-day culture period.

2.5. Evaluation of Compatibility between Adipose Stem Cells and Collagen Hydrogel

Using the Live/Dead® Cell Viability Assay Kit (No.1) (R37601, Life Technologies, Carlsbad, CA, USA), the viability of adipose-derived stem cells embedded in hydrogels was evaluated after 24 hours. The assay was conducted based on the instructions provided by the manufacturer. Hydrogels were incubated with dye in a 4-well plate for 15minutes at room temperature in the dark.Subsequently, the hydrogels were washed with PBS and finally immersed in PBS for observation and image acquisition under a microscope.

2.6. Influence of Hydrogel Matrix Stiffness on Adipocyte Proliferation

To assess the impact of matrix stiffness on adipocyte proliferation within 3D hydrogels, four hydrogels from each concentration group were randomly chosen and placed in 1.5 ml centrifuge tubes. Add 100 μL of 0.2% collagenase I solution to each tube and incubate in a 37 °C water bath for 30 minutes. Post-digestion, samples were centrifuged at 2000 rpm for 5 minutes, and the supernatant was discarded. The Cell Counting Kit-8 (CCK-8) reagent was diluted 1:10 with serum-free DMEM medium. Subsequently, 100μL of CCK-8 mixture was added to each sample and incubated at 37°C for two hours.Finally, measure the absorbance at 450nm with a microplate reader to determine the peak value of cell proliferation and perform statistical analysis.

2.7. Quantification of Lipid Accumulation in ADSCs Using BODIPY

Staining

To quantify intracellular lipid accumulation, we used BODIPY 493/503 lipid staining reagent (MCE) to fluorescently label lipids. The cultured hydrogels were first fixed for 10 minutes in 4% paraformaldehyde (PFA). The samples were washed thrice with phosphate-buffered saline (PBS) for 5minutes each and then permeabilized with 0.2%Triton X-100 for 15 minutes at room temperature. The samples were washed three times with PBS for five minutes per wash.Cells were stained with 5μM BODIPY for 15 minutes and then washed three times with PBS. Cell nuclei were stained with

 doi:10.20944/preprints202410.0446.v1

2ng/mL DAPI for 15minutes, followed by a PBS wash. Fluorescence microscopy was employed for imaging, and ImageJ software quantified intracellular green fluorescence indicative of lipid droplets. Statistical analyses were conducted using GraphPad Prism 8 software.

2.8. Real-Time PCR Quantitative Analysis

Following digestion with 0.2%type I collagenase for 30minutes, cells were centrifuged and total RNA was isolated using TRIzol reagent (Ambion). cDNA was generated using Bio-Rad's iScript cDNA Synthesis Kit. A qRT-PCR program was conducted using the StepOne Plus Real-Time PCR System (Applied Biosystems) and the SensiMix SYBR Hi-ROX kit (QT-605-05, Bioline).Table 1provides a list of primers used.

Table 1. RT-PCR Primer.

Target	Forward primer (3′-5′)	Reverse primer (5′-3′)
GAPDH	**GCATCTTCTTGTGCAGTGCC**	**GATGGTGATGGGTTTCCCGT**
LPL	**GAGAAGGGGCTTGGAGATGT**	**ATGCCTTGCTGGGGTTTTCT**
ADIPOQ	**CCGTTCTCTTCACCTACGAC**	**TTCCCCATACACTTGGAGCC**
PPARa	**TCGTGGAGTCCTGGAACTGA**	**CTTCAGTCTTGGCTCGCCTC**
FABP-4	**AGAAGTGGGAGTTGGCTTCG**	**ACTCTCTGACCGGATGACGA**

2.9. Measurement of Changes in Hydrogel Diameter after Cell Seeding

After the cells were inoculated into the hydrogel, the hydrogel was removed from the silicone mold after solidification. A standard ruler was used as a scale for the size of the hydrogel (See Supplementary Data S2) and the diameter change of the cell hydrogel was measured at 6, 12, 24, and 48 hours after inoculation. The contraction data of the hydrogel at different time periods were recorded in detail. Five data sets per concentration were measured and analyzed statistically using GraphPad 8.

2.10. YAP Immunofluorescence Staining

After 9 days, cells were fixed in 4% PFA for 15 min, washed three times in PBS for 5 min each, permeabilized with 0.2%Triton X-100 for 10 min, and washed again three times in PBS for 5 min each. Next, we blocked non-specific binding with 5%BSA for 60min.The YAP antibody (Santa Cruz Biotechnology, sc-101199) was diluted 1:200 and incubated at 4°C overnight.The following day, we performed three 10-minute PBS washes to eliminate unbound primary antibodies. Fluorescently labeled secondary antibodies were diluted 1:1000 and incubated in the dark for 1 hour. Nuclei were stained by a DAPI solution of 1μg/ml for 5-10minutes at room temperature. Finally, we washed three times with PBS for 5min each. Images were taken with a confocal microscope for the observation of YAP localization, in which nuclei are stained blue by DAPI, YAP is stained in green by Alexa Fluor 488. Images were merged for further analysis.

2.11. Western Blot

The cells were extracted from the hydrogels according to previously established methods. Cells were lysed on ice for 30 minutes using protease and phosphatase inhibitors (HaltTM Protease and Phosphatase Inhibitor Cocktail, 100X, Thermo Scientific, USA; EBA-78440, ELPIS Biotech, South Korea). Protein concentrations in the supernatant were measured using the Pierce BCA Protein Assay Kit (Thermo Scientific) after centrifugation at 10,000rpm for 10minutes at 4°C, according to the manufacturer's instructions. Samples were heated at 100°C for 10minutes to denature them before separation via SDS-PAGE.Protein electrophoresis was followed by transfer to PVDF membranes. The membranes were blocked with BSA (SolMate BSA Grade IY, GeneAll) for 60 minutes, then incubated overnight at 4°C with primary antibodies against phospho-YAP and GAPDH. Following three TBST washes the next day, the membrane was incubated with HRP-conjugated antibody for 1hour. Protein signals were captured using the LAS4000mini protein imaging system (Sweden) with Supersignal

 doi:10.20944/preprints202410.0446.v1

West Pico and Supersignal West Pico PLUS Chemiluminescent Substrates (Thermo Scientific). Quantitative analysis was conducted using ImageJ software. Table 2 provides a list of primers used.

Table 2. Antibody statistics.

Antibody	Company	Item number	Attributes	Dilution ratio
Phospho-YAP	Cell Signaling	4911	Rabbit	1:1000
YAP	Cell Signaling	14074S	Rabbit	1:1000
GAPDH	Santa Cruz Biotechnology	SC-47724	Mouse	1:500

2.12. Porosity Analysis of Freeze-Dried Hydrogels

After preparing the cell-free hydrogel samples, they were subjected to rapid freezing in liquid nitrogen followed by freeze-drying. Platinum (Pt) was sputter-coated onto the freeze-dried hydrogels using a Japanese sputter coater, the Eiko IB-3. A scanning electron microscope (JEOL-SEM 3000, Japan) operated at 5kV acceleration voltage was then used to determine the porosity of the freeze-dried hydrogels. The physical support provided by the porous structure was evaluated, and the influence of cross-sectional pore size on cell differentiation was investigated. Finally, quantitative analysis of pore size distribution was conducted using Nano Measurer 1.2 software.

2.13. Effects of YAP Inhibition on Lipid Droplets in Hydrogels

This experiment aims to investigate the effect of verteporfin (VP), an inhibitor of the YAP signaling pathway, on lipid droplet formation in hydrogels. On day 7 of differentiation, hydrogels were treated with 1μM verteporfin (VP). Two experimental groups were formed: a control group and a YAP inhibition group with an inhibition time of 48 hours. Four randomly selected hydrogels were used in each experimental group. These experiments involved the use of BODIPY staining to assess lipid droplets in normal and suppressed groups.

3. Results

3.1. From Tissue to Hydrogel: Constructing an In Vitro Model for Accurate Simulation of the Microenvironment for Adipocyte Differentiation

To accurately simulate the microenvironment of adipocyte differentiation in vitro, we first extracted samples from rat inguinal adipose tissue and measured the stress and elastic modulus at different sites. These tests provided mechanical property benchmarks, including stress and elastic modulus, of real adipose tissue for the in vitro model.

The rat inguinal adipose tissue is strip-shaped with the thickness ranging from thin to thick. We further divided the entire adipose tissue into three parts: ATP, MPT, and PPT (Figure 1A), and then tested stress and elastic modulus of each part. Results demonstrated that, from the ATP to the PPT, both stress and elastic modulus showed a gradual increase. Figure 1B illustrates this. For these samples, the compressive stress values were measured as 294.6±41Pa for ATP, 606.3±90.7Pa for MPT, and 1013.6±89Pa for PPT. Under strain conditions of 60%, elastic modulus was determined as 589.2±81.9Pa for ATP, 1212.7±181.6Pa for MPT, and 2027.2±178Pa for PPT (Figure1A,B,C). These differences could be due to a variance in thickness and cell density within the specimen of adipose tissue, since thicker sections contain more adipocytes, therefore higher cell-cell mechanical interactions and thus an elastic modulus. Thinner sections would consequently carry more connective tissue or blood vessels, which have a lower elastic modulus.

Using these data, we formulated hydrogels at concentrations of 0.5 mg/ml, 1mg/ml and 2mg/ml to replicate varying mechanical environments. Corresponding hydrogel stress and elastic modulus were 344Pa, 982Pa, and 1220Pa, and 301.8±43.9Pa, 1561±98.6Pa, and 2250.58±89.62Pa, respectively, which closely approximate the mechanical properties of in vivo adipose tissue. This design created an in vitro environment mimicking in vivo conditions to study the impact of hydrogel mechanical properties on adipocyte differentiation.

 doi:10.20944/preprints202410.0446.v1

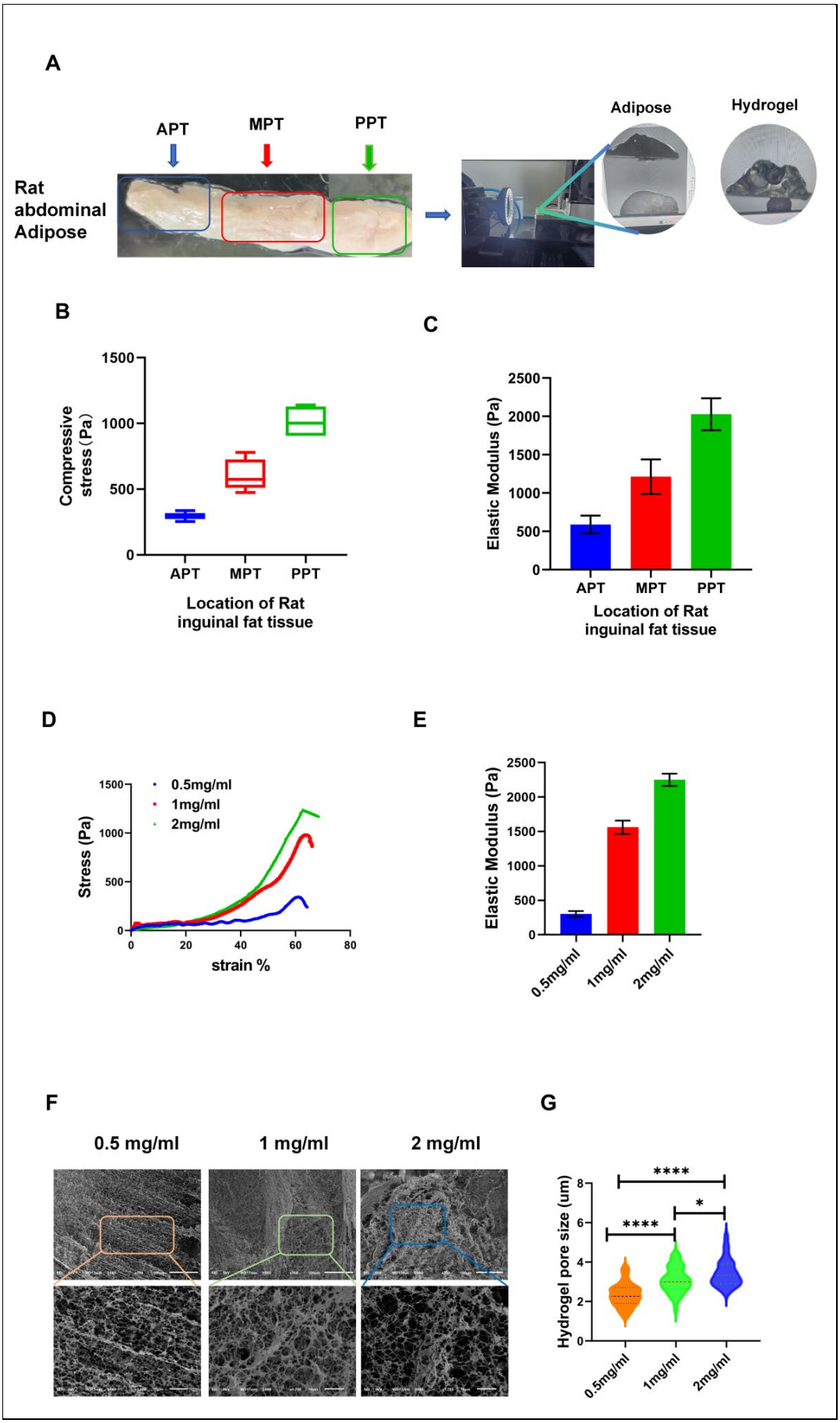

 doi:10.20944/preprints202410.0446.v1

Figure 1. Mechanical Properties of Adipose Tissue and Physical Characteristics of Hydrogels at Different Concentrations. (A) Results of stress and elastic modulus tests on different regions of adipose tissue. (B) Statistical results of stress testing in adipose tissue. (C) Testing results of the elastic modulus in various regions of adipose tissue. (D) Stress testing results of hydrogels at different concentrations. (E) Elastic modulus testing results of hydrogels at varying concentrations. (F) Scanning electron microscopy (SEM) images of hydrogels at different concentrations. (G) Statistical analysis of pore sizes in hydrogels at different concentrations. APT (Anterior Part of the Adipose Tissue) MPT (Middle Part of the Adipose Tissue) PPT(Posterior Part of the Adipose Tissue). The pore diameters were analyzed using Nano Measurer 1.2 software and statistically processed using GraphPad software. ** $p < 0.01$, *** $p < 0.001$, NS not significant.

Adipose tissue's microenvironment and the stiffness of hydrogels support the cellular processes of cell proliferation, differentiation, and migration. On the other hand, equally important to cell survival is the exchange of substances between cells and their immediate surroundings, a process in which the pore structure of hydrogels acts as a determining factor. Pore size directly affects the uptake of external nutrients by cells and regulates cellular behavior at both physical and chemical levels.Therefore, in hydrogels, the pore structure may significantly contribute to the imitation of an in vivo environment and further affect cell differentiation.

These may involve mechanical properties like stiffness, viscoelasticity, and porosity. How cells perceive and respond to such mechanical signals is referred to as mechanotransduction. Mechanotransduction converts forces into biochemical signals, altering cell behavior by activating intracellular signaling pathways, regulating gene expression, and modifying cell shape and cytoskeletal organization [26–28]. To further investigate the pore characteristics of hydrogels at different concentrations, freeze-dried hydrogel analysis was conducted using SEM. Results are presented in (Figure 1F,G). The results indicated that pore size increased with concentration. Hydrogels containing 0.5mg/mL, 1mg/mL and 2mg/mL measured 1.5-3 μm, 2-4 μm, and 2.5-5 μm, respectively. The pores in 0.5 mg/mL were concentrated between 1.8-2.5 μm; for the 1 mg/mL hydrogel, pores in this concentration were located within a range of 2-3.5 μm, and the majority of pores in the 2mg/mL hydrogel were between 2.8-4.7 μm.

The large pores in a 2mg/mL hydrogel, ranging between 2.5 and 5 μm, are capable of exchanging more nutrients between the cells and their environment while providing space for cell migration and growth. Similarly, such large pores enhance the capability of mechanical sensing by cells inside the matrix, thus enhancing cell-hydrogel interaction. Cells have been shown in previous literature to modulate their differentiation processes via sensing the mechanical properties and pore structure of the matrix.Larger pores in 2mg/mL hydrogel could be more favorable in a microenvironment for differentiation. Compared to the lower concentration hydrogels (0.5 and 1mg/mL), 2mg/mL hydrogel possesses higher compressive stress and elastic modulus, while the pore structure is larger, which may be more conducive to nutrient uptake and the reception of differentiation signals. This means that this pore size and cell differentiation are related, thus providing a distinct advantage for 2mg/mL hydrogels to promote the differentiation of adipocytes.

3.2. Fluorescent Staining of Lipid Droplets in 3D Hydrogels (BODIPY)

In a 3D environment, different concentrations of collagen hydrogel significantly affected the ability of adipogenic stem cells (ADSCs) to differentiate into adipocytes. This observation was confirmed by BODIPY staining after 9days of differentiation, as shown in (Figure 2A,B). Compared to other concentration groups, more green fluorescent lipid droplets were observed in the 2mg/mL hydrogel. The fluorescence intensity of lipid droplets in the 2mg/mL hydrogel increased by 30.44% compared to the 0.5mg/mL hydrogel, promoting lipid accumulation and facilitating ADSC differentiation into mature adipocytes.Compared to the 1mg/mL hydrogel, the fluorescence expression of lipid droplets in the 2mg/mL hydrogel increased by 17.74%. BODIPY staining demonstrates that the 2mg/mL hydrogel significantly enhances lipid droplet accumulation and adipocyte differentiation, indicating a more favorable microenvironment for adipocyte phenotype development. Under 3D culture conditions, the 2mg/mL collagen hydrogel is particularly suitable for

 doi:10.20944/preprints202410.0446.v1

promoting the adipogenic differentiation of ADSCs into mature adipocytes. 3D multilayer fluorescent images depicting the differentiation of mature adipocytes. (See Supplementary Figure S3 for details). These observations suggest that the 2mg/mL concentration of collagen hydrogel provides the optimal scaffold structure and biological microenvironment for promoting the adipogenic differentiation of ADSCs.

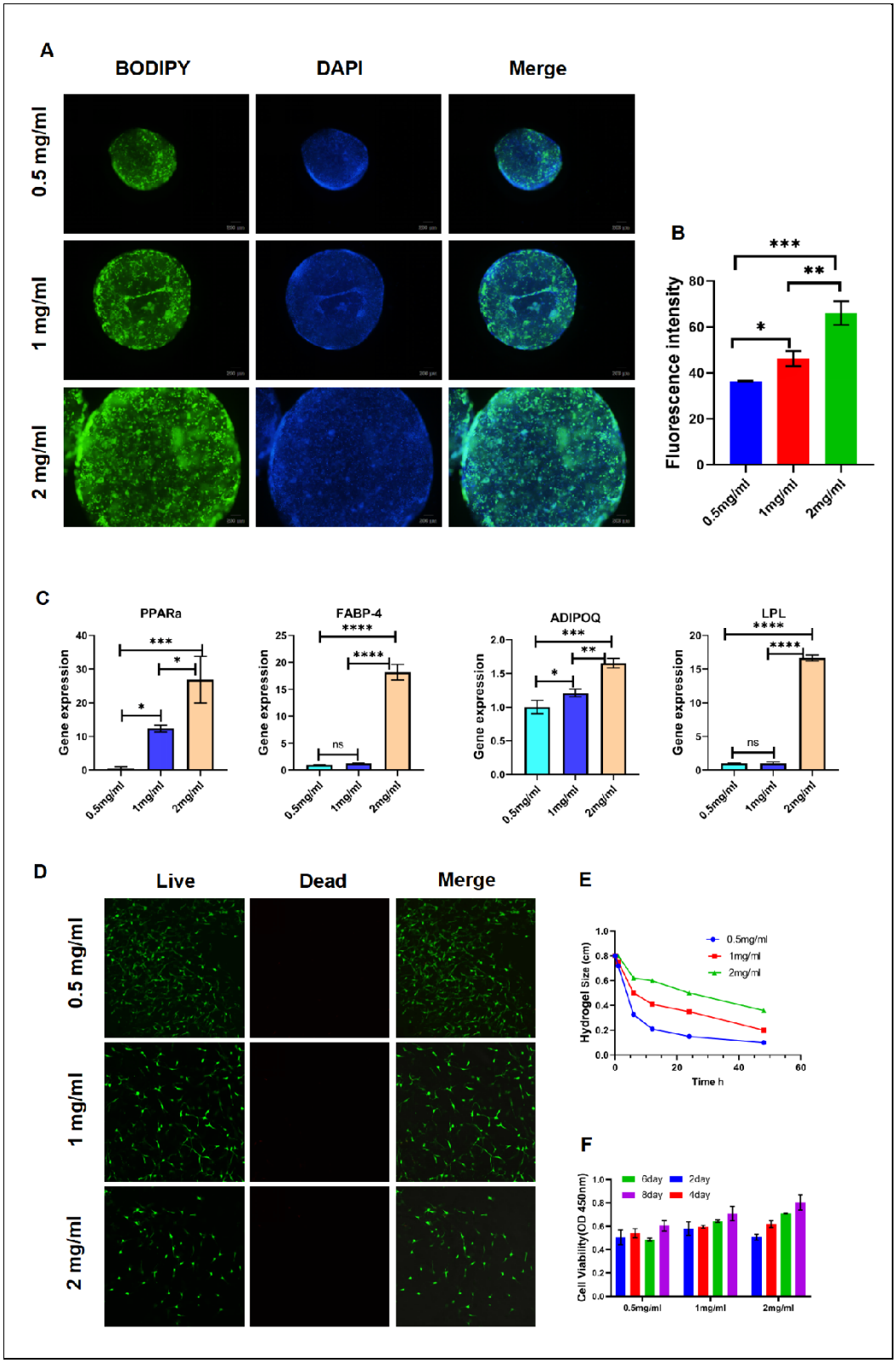

Figure 2. Comprehensive Assessment of the Effects of Hydrogels on Adipocyte Function and Material Mechanical Properties (A) Observation of adipocyte differentiation in hydrogels via fluorescence

 doi:10.20944/preprints202410.0446.v1

staining. (B) Quantitative analysis of fluorescence signals related to adipocyte differentiation. (C) Measurement of the expression levels of specific genes associated with adipocyte differentiation. (D) Evaluation of adipocyte viability within the hydrogels. (E) Assessment of the impact of cell embedding on hydrogel contraction. (F) Monitoring of cell proliferation in hydrogels over different culture time periods.Fluorescence intensity was analyzed using ImageJ software and statistically processed using GraphPad software. ** $p < 0.01$, *** $p < 0.001$, NS not significant. (Scale bar in figure A:200μm,D :100 μm).

3.3. Adipocyte Marker qRT-PCR Analysis

The stiffness of the matrix differentially affects specific adipogenic genes. LPL, ADIPOQ, PPARa and FABP4 were detected to be differentially expressed during adipocyte differentiation through qRT-PCR analysis. (Figure 2C) illustrates a significant 1.65-fold increase in ADIPOQ gene expression in the 2mg/mL hydrogel compared to the 0.5mg/mL concentration. FABP4 expression levels and LPL and PPARG genes in the 2mg/mL hydrogel increased by 18.17-fold, 16.65-fold, and 26.366-fold, respectively, compared to the 0.5mg/mL concentration.The expression levels of LPL, ADIPOQ, PPARG and FABP4 genes in adipose-derived stem cells (ADSCs) were significantly elevated in a 2mg/mL collagen hydrogel, suggesting that this concentration fosters a conducive microenvironment for adipocyte differentiation and enhances the transcription of these adipocyte-related genes.

3.4. Cytotoxicity Test

Cell viability and survival status were assayed using a live/dead cell staining kit. Staining was at room temperature for 15 min, after which cells were washed again with PBS to remove extra dye. The stained hydrogels were then observed under a confocal microscope-record of cell morphology and distribution is shown in (Figure 2D). Through the experimental results, it can be observed that there was no obvious cell death in the hydrogel after 24 hours of culture. This indicated that the hydrogel culture condition had a good effect on cell survival and activity. Moreover, live cells distributed uniformly within the gel without morphological changes characteristic for apoptosis or necrosis.

3.5. Cell-Mediated Shrinkage of Hydrogels

Cells interact with hydrogels through mechanical and chemical signals to regulate their morphology and function.Hydrogels mimic the extracellular matrix (ECM), providing cells with a scaffold on which they can exert traction, leading to compaction and contraction of the gel. These force interactions are co-regulated by mechanical and chemical signaling pathways between cells and hydrogels. As shown in (Figure 2E), in our study, we conducted hydrogel contraction experiments to assess the behavior of adipocytes within the hydrogel matrix. These experiments were conducted at different time points (6hours, 12hours, 24hours, and 48hours) to study the contraction phenomenon of adipocytes cultured in hydrogels of different concentrations. The hydrogels were placed under specific conditions, and their contraction rates were measured periodically. Our research results show varying degrees of hydrogel contraction.After 48 hours of culture and contraction, compared with the initial size of 0.8cm, the 0.5mg/mL hydrogel shrank by 87.5%, the 1 mg/mL hydrogel shrank by 75%, and the 2mg/mL hydrogel shrank by 55%. The concentration of the hydrogel significantly influenced adipocyte contraction behavior. When the same number of cells were embedded in hydrogels of different concentrations, the cells' perception of the microenvironment depended on the change in matrix stiffness, which caused the difference in contraction of hydrogels of different concentrations. In hydrogels of different concentrations with the same cell encapsulation, cell perception of the microenvironment depends on changes in substrate stiffness.

3.6. Cell Viability and Proliferation

Biocompatibility is a crucial factor to prioritize in the application of biomaterials. In our experiment (Figure 2F) we embedded adipose-derived stem cells (ADSCs) in hydrogels of varying

 doi:10.20944/preprints202410.0446.v1

concentrations and assessed their survival and proliferation at 2, 4, 6, and 8 days. The results showed that cells maintained a high survival rate in hydrogels of all concentrations, with a notable proliferation trend over time. Notably, in the 2mg/ml concentration of hydrogel, cell proliferation exhibited a gradient increase with time. As the concentration of the hydrogel increased, there was also a significant gradient change in the proliferation rate and distribution of cells.This indicates that hydrogel concentration not only impacts the survival of adipose-derived stem cells but also modulates their proliferation behavior to some extent. These results underscore the importance of hydrogels as cell culture matrices, highlighting that they must possess good biocompatibility and that their physicochemical properties should be optimized according to different application needs to regulate cell behavior effectively.

3.7. Modulation of YAP Function and Localization by Hydrogel Stiffness

Extracellular matrix stiffness is a key mechanical factor in regulating YAP activity [29]. (Dupont et al.) Found that increased matrix stiffness promotes the nuclear localization and activity of YAP [30]. However, our results appear to contrast with this finding, which may reflect the specific response of adipocytes to mechanical stimuli.In fact, (Calvo et al.) Reported that in mammary epithelial cells, high-stiffness matrices promote the cytoplasmic retention of YAP [31], aligning with our observations in adipocytes.

Moreover, increasing the concentration of hydrogels not only alters the matrix stiffness but may also affect cell-matrix interactions and nutrient diffusion [32]. These factors, working in concert, could modulate YAP activity and the adipocyte differentiation process through multiple signaling pathways. Rho GTPases and the actin cytoskeleton are crucial in regulating YAP activity through mechanical forces [33], suggesting a potential direction for future research.

Our experimental results demonstrate that the concentration of hydrogels significantly affects the intracellular localization and activity of Yes-associated protein (YAP), thereby regulating the differentiation process of adipocytes.Through fluorescence colocalization analysis, we assessed the localization of YAP in the nucleus and its overlap with nuclear regions.Increasing the hydrogel concentration from 0.5mg/ml to 2mg/ml significantly altered the shuttling behavior of YAP between the nucleus and cytoplasm (Figure 3A–C). The 0.5mg/ml hydrogel exhibited the highest YAP nuclear localization, with YAP predominantly translocating to the nucleus in this softer microenvironment. The overlap rate between YAP and the nucleus was 69.44% ± 13.08%.As the hydrogel concentration increased, YAP's nuclear localization gradually decreased.In the 1 mg/ml hydrogel, the overlap rate between YAP and the nucleus was 60.24% ± 10.6%, while in the 2mg/ml hydrogel, this value dropped to 34.54% ± 11.08%, indicating that the activation of YAP nuclear localization is negatively correlated with the hydrogel concentration.At higher hydrogel concentrations, YAP remains largely inactive, predominantly residing in the cytoplasm (Figure 3C). In the cytoplasm, YAP fluorescence intensity significantly increased with the stiffness of the hydrogels, suggesting that YAP was unable to translocate to the nucleus. The cytoplasmic retention of YAP in hydrogels was 30.56%±9.48% for 0.5mg/ml, 39.8%±8.84% for 1mg/ml, and 65.46%±9.48% for 2mg/ml. These data further demonstrate that YAP activation is dependent on the mechanical stiffness of the hydrogels.

In the fluorescence colocalization experiment (Figure 3D), we focused on analyzing the nuclear distribution of YAP in hydrogels of varying concentrations. The results showed that as the hydrogel concentration increased, the distribution of YAP within the nucleus gradually decreased, indirectly supporting the conclusion that YAP nuclear translocation is regulated by the stiffness of the hydrogels. Notably, after YAP enters the nucleus, it typically cooperates with transcription factors to regulate gene expression, thereby influencing cell proliferation and differentiation.On the other hand, when YAP predominantly remains in the cytoplasm, its retention is often associated with the promotion of mature adipocyte differentiation. To further verify whether hydrogel concentration is a key factor influencing YAP nuclear translocation, we performed Western Blot (WB) analysis, which corroborated these findings. We measured the expression of YAP protein in hydrogels of different concentrations (Figure 3F–I). The results indicated that with increasing hydrogel concentration, YAP expression in the nucleus significantly decreased, while its expression in the cytoplasm increased

 doi:10.20944/preprints202410.0446.v1

accordingly. This aligns with prior findings on YAP nuclear translocation, indicating that hydrogel concentration influences both YAP intracellular localization and its protein expression. YAP, a crucial effector in the Hippo signaling pathway, is pivotal in mechanotransduction and cell fate determination [34]. Previous research indicates that the nuclear localization of YAP, an active form, enhances stem cell proliferation and suppresses differentiation [35]. Our experimental findings further reveal the significant impact of hydrogel concentration on the intracellular localization and activity of YAP. YAP progressively translocated from the nucleus to the cytoplasm as the hydrogel concentration increased from 0.5mg/ml to 2mg/ml. In the low-concentration hydrogel (0.5mg/ml), YAP primarily accumulated in the nucleus, whereas at higher concentrations (2mg/ml), YAP was predominantly retained in the cytoplasm. YAP nuclear localization and protein expression levels decreased as hydrogel concentration increased, highlighting the significant role of hydrogel mechanical stiffness in regulating YAP nuclear translocation and adipocyte differentiation. This phenomenon was confirmed through fluorescence colocalization experiments and Western Blot protein expression analyses, further supporting the regulatory effect of hydrogel stiffness on YAP activity and adipocyte differentiation.

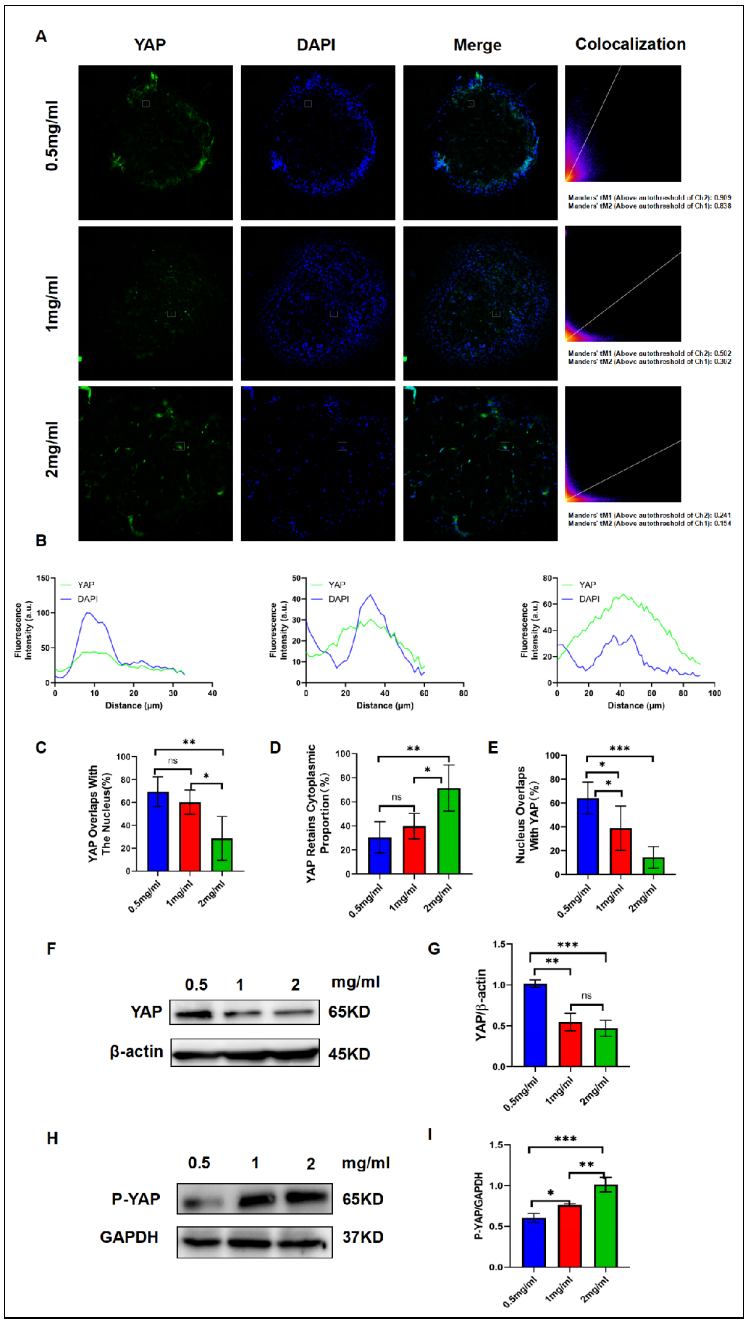

 doi:10.20944/preprints202410.0446.v1

Figure 3. Immunofluorescence Co-localization and Protein Analysis of YAP Expression in Hydrogels. (A) Immunofluorescence staining of YAP in adipocytes cultured in hydrogels of different concentrations. YAP is shown in green, and the nucleus is stained with DAPI (Blue), with the merged images displaying co-localization.In the histogram, the red represents YAP signals (green fluorescence channel), while the blue represents DAPI signals (nuclei). (B) A single cell is outlined as the test subject, as shown in Figure 3A. The nucleus is labeled with DAPI (Blue) and YAP is labeled in green, outlined by a white line.The fluorescence intensity distribution of YAP and DAPI along the white box is analyzed, with the intensity values normalized to the average YAP intensity. (C) Percentage of YAP co-localized with the nucleus. (D)Proportion of YAP signals not overlapping with the nucleus. (E) Percentage of YAP localized within the nucleus. (F) Western blot analysis of YAP protein expression in varying hydrogel concentrations. (G) Quantitative analysis of YAP protein expression across varying hydrogel concentrations. (H) Western blot analysis of phosphorylated YAP (P-YAP) protein expression in hydrogels of different concentrations. (I) Quantitative analysis of P-YAP protein expression across various hydrogel concentrations was conducted. Fluorescence intensity and co-localization data were processed with ImageJ software, and statistical analysis was executed using GraphPad software.Statistical significance is indicated as $^{**}p < 0.01$, $^{***}p < 0.001$ and NS for not significant. (The scale bar in Figure A represents 100 μm).

3.8. Inhibiting YAP Promotes Adipogenesis

YAP is an important transcriptional coactivator that controls the process of differentiation into adipocytes.Indeed, various publications have documented that the inhibition of YAP promotes the differentiation of adipocytes. It has been indicated that dysfunctional adipocytes trigger YAP/TAZ signaling through a process that leads to dedifferentiation and tumor development.Inhibition of YAP/TAZ in these models restored the function of the adipocytes and diminished inflammation, thus suggesting that targeting YAP improves adipocyte differentiation [36]. Further research indicates that YAP repression promotes the differentiation of other cell types, including endothelial cells, by inducing key transcription factors such as FLI1. These findings suggest that YAP repression may play a broader role in promoting the differentiation of multiple cell types into adipocytes [37]. YAP, in relation to myxoid liposarcoma, represses adipogenic differentiation; hence, inhibition of YAP should reverse this effect, promoting normal adipocyte differentiation [38].

Previous research indicates that YAP signaling regulates lipid droplet accumulation, with expression levels directly affected by matrix stiffness. We inhibited YAP signaling to investigate its impact on lipid droplet accumulation in hydrogel-induced adipogenesis.After inhibiting YAP signaling for 48hours, we stained the lipid droplets with BODIPY and analyzed the fluorescence intensity using ImageJ software. The results, as depicted in (Figure 3A), indicated that lipid droplet accumulation in the control group was consistent with the observations in (Figure 2A). Inhibition of YAP signaling led to increased lipid droplet accumulation in the inhibited group's hydrogel compared to the control group. Statistical analysis of (Figure 3B) reveals that the inhibition group exhibited higher fluorescence intensity compared to the control group, suggesting that inhibiting YAP signaling, which retains YAP in the cytoplasm, enhances lipid droplet accumulation. This was corroborated by BODIPY staining of lipid droplets in various hydrogels, confirming that YAP signaling pathway inhibition promotes lipid droplet accumulation. As shown in（Figure 3B,D,E） Western blot (WB) experiments also corroborate this finding.In the WB experiments, inhibiting the YAP signaling pathway with VP led to increased protein expression compared to the non-inhibited pathway. Matrix stiffness impacts YAP expression, which subsequently influences lipid droplet accumulation, highlighting YAP's essential role in adipogenesis.

 doi:10.20944/preprints202410.0446.v1

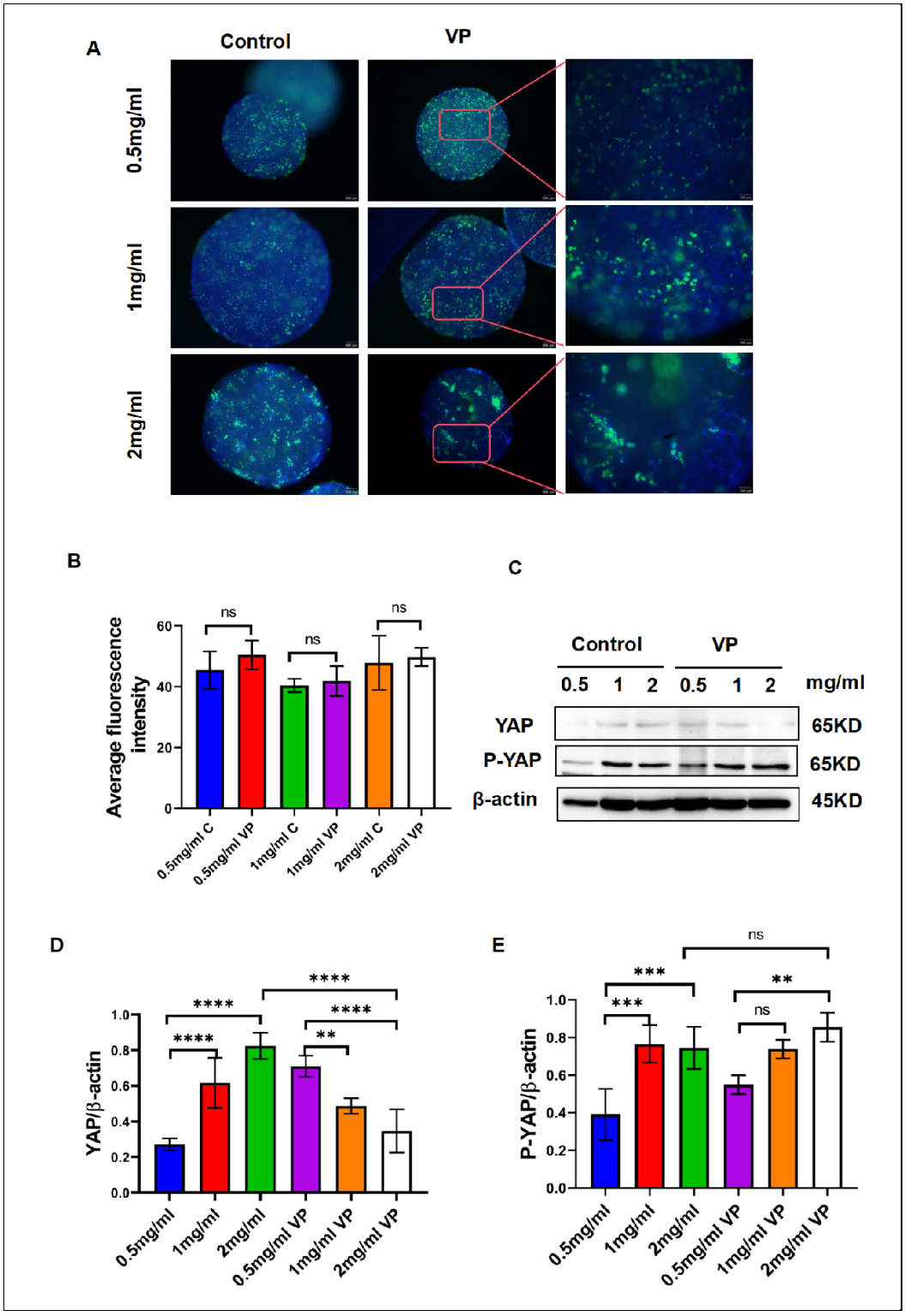

Figure 4. Inhibition of the YAP Signaling Pathway Promotes Adipogenesis. (A) BODIPY fluorescence staining of lipid droplets following inhibition of the YAP signaling pathway using the VP inhibitor. (B) Fluorescence intensity analysis of lipid droplets in hydrogels of different concentrations. (C) Changes in YAP/P-YAP protein levels after VP inhibition. (D,E) Quantitative analysis of protein expression changes after YAP signaling inhibition.The fluorescence intensity in Figures (A) and (C) was analyzed using ImageJ software, and statistical data was processed using GraphPad software.Statistical significance is denoted as ***p < 0.001, **p < 0.01, and ns for non-significant differences.(Scale bar in Figure A: 200 μm).

 doi:10.20944/preprints202410.0446.v1

3.9. Hydrogel Concentration Regulates Adipocyte Migration Behavior

Hydrogel concentration significantly influences adipocyte migration and behavior, particularly through its mechanical properties and matrix density. Research indicates that the stiffness and density of hydrogels can regulate the phenotype and migration dynamics of adipocytes. Mechanical characteristics, such as stiffness, affect adipocyte migration, where softer hydrogels often promote different migration strategies compared to stiffer ones, thus impacting the overall behavior of adipocytes [39] .

The co-culture system validated the impact of hydrogel concentration on adipocyte differentiation and migration, revealing changes in YAP activity and migration patterns in hydrogels at 0.5mg/ml, 1mg/ml, and 2 mg/ml. Hydrogel concentration clearly had an impact on intracellular localizations and activity of YAP, further influencing the differentiation and migratory capacity of adipocytes. The differentiation and migration of adipocytes in hydrogels of different concentrations were studied in the co-culture system, in which an upper chamber with 8μm pores was placed in a lower 24-well plate (Figure 5B). The observations at the bottom of the 24-well plate after 9days of differentiation were described in (Figure 5C) under the 2mg/ml conditions of hydrogel, a few cells could migrate to the bottom of the plate, while no cell migration was found under the 0.5 mg/ml and 1 mg/ml conditions. (Figure 5A) demonstrates cell migration across all tested hydrogel concentrations at the bottom of the 8μm pore chamber, with a significant increase in migrating cell numbers corresponding to higher hydrogel concentrations. The 2mg/ml hydrogel condition yielded the highest number of migrating cells.

These findings point out that hydrogel concentration, or matrix stiffness, has a great influence on the differentiation and migration of adipocytes.Previous studies indicate that the matrix's physical properties, particularly stiffness, significantly affect cellular behaviors like differentiation and migration [40]. Our findings align with previous studies and emphasize the critical role of matrix stiffness in adipocyte differentiation. Moreover, we found that even when the cells could migrate through the 8μm pores, they only reached the bottom of the 24-well plate under the condition of 2mg/ml. This indicated that matrix stiffness might influence not only the tendency for the cell to migrate but also their ability and persistence.

 doi:10.20944/preprints202410.0446.v1

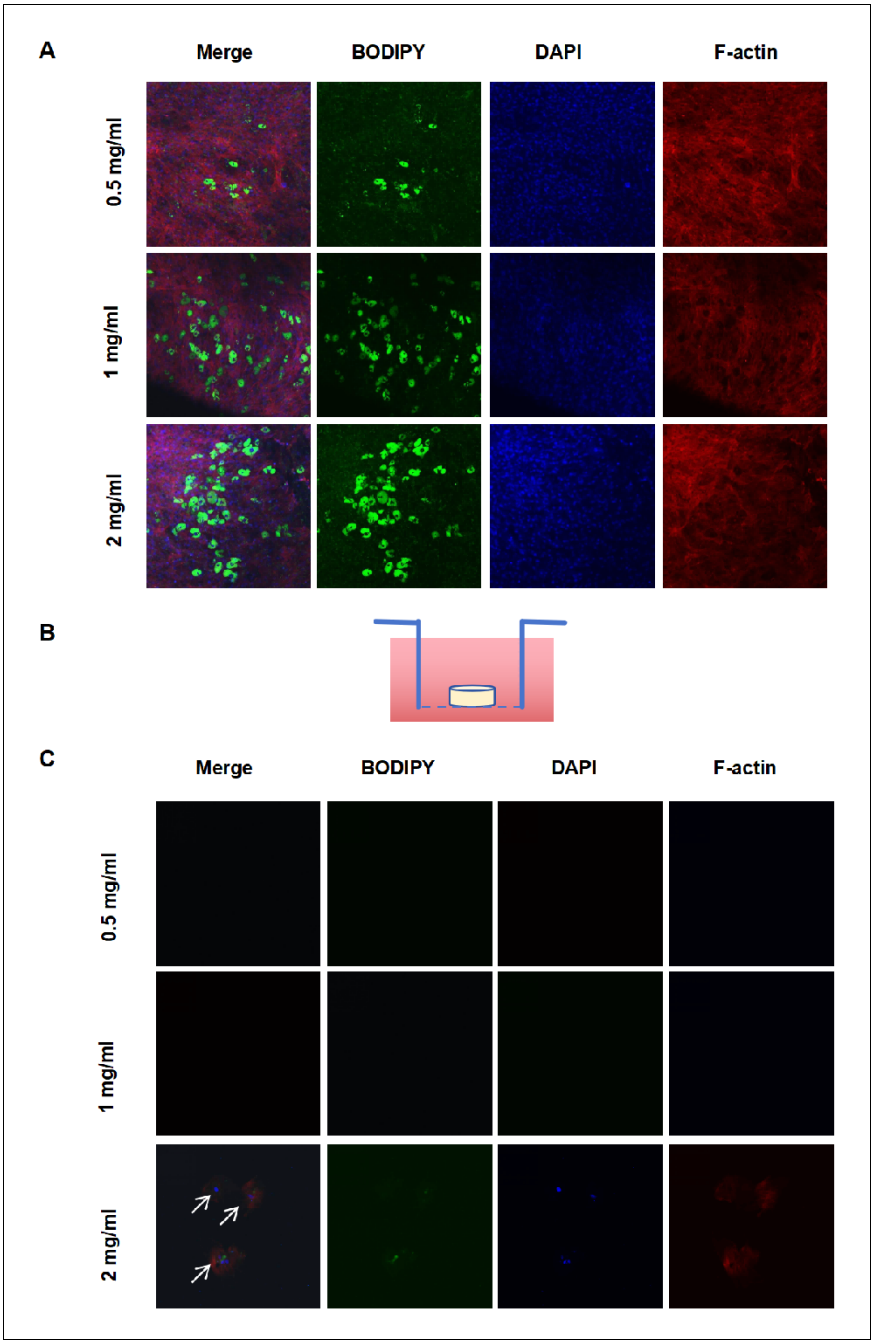

Figure 5. Effect of hydrogel stiffness on adipocyte migration . (A) Cell staining at the bottom of the 8μm pore size chamber, showing adipocyte migration characteristics in hydrogels of different concentrations. Schematic diagram of the co-culture system featuring an 8 μm pore size upper chamber and a lower 24-well plate for observing cell migration behavior. (C) Cell migration in the bottom of the 24-well plate, with lipid droplets stained green using BODIPY and actin filaments stained red using fluorescence staining.Fluorescence intensity was analyzed using ImageJ software and statistically processed using GraphPad software. ** $p < 0.01$, *** $p < 0.001$, NS not significant.(Scale bar in figure B ,C: 100 μm).

3.10. Hydrogel Stiffness Modulates YAP-Mediated Adipocyte Differentiation

During differentiation, cells are influenced by mechanical forces from hydrogels of varying hardness, and YAP exhibits differential sensitivity to these forces. Mechanical force enables YAP to move between the nucleus and cytoplasm. (Figure6) illustrates that in softer hydrogels, YAP less frequently shuttles from the nucleus to the cytoplasm, leading to reduced phosphorylation and decreased lipogenesis. In the harder hydrogel, increased YAP shuttling from the nucleus to the

 doi:10.20944/preprints202410.0446.v1

cytoplasm and subsequent phosphorylation result in higher lipogenesis compared to the softer hydrogel. In summary, stiffer hydrogels are more conducive to fat differentiation.

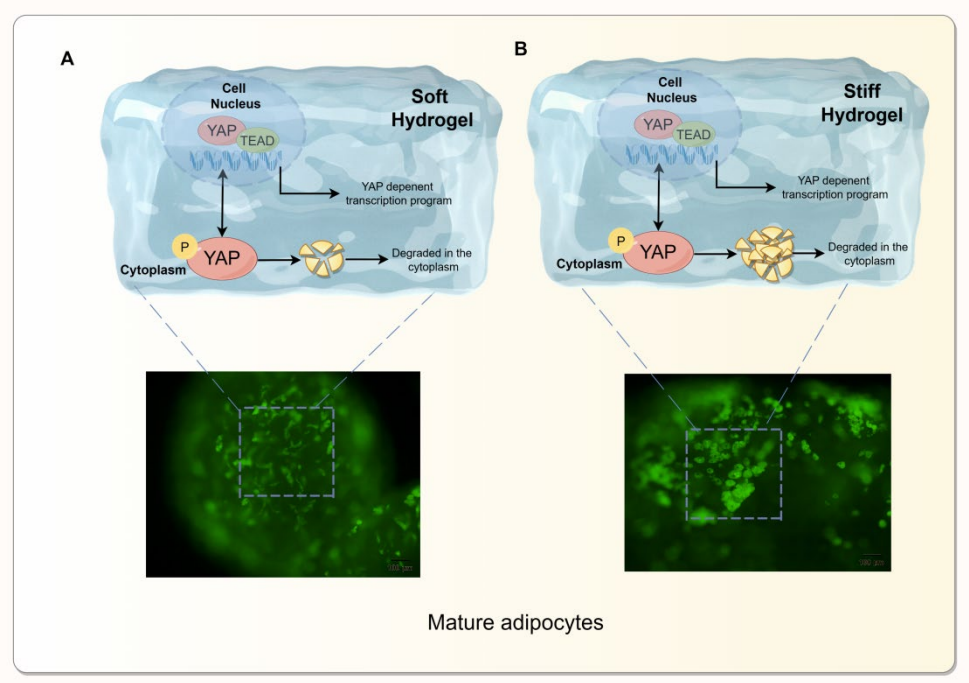

Figure 6. Adipocyte differentiation is regulated by the YAP signaling pathway. (A ,B) show collagen hydrogels of different stiffness.In the softest hydrogels (A) YAP transfer from the nucleus to the cytoplasm is diminished, resulting in minimal lipid droplet accumulation.In the stiffer hydrogel (B) the increased phosphorylation level of YAP promotes the accumulation of large lipid droplets. Hydrogels with varying matrix hardness influence YAP relocalization between the nucleus and cytoplasm under mechanical force. If YAP remains in the cytoplasm, it is phosphorylated, which promotes initiation of the adipocyte differentiation program. Therefore, matrix stiffness ultimately affects the differentiation process of adipocytes by regulating the cellular location and activity state of YAP.

4. Discussion

The present study has systematically investigated how collagen hydrogels of different stiffnesses affect the differentiation of ADSCs and then disclosed the regulatory function of YAP signaling in such a process. The gain in hydrogel stiffness was found to significantly enhance the adipogenic differentiation capability of ADSCs, which is documented by increased number and size of lipid droplets as well as remarkably higher mRNA expression of adipocyte-specific genes like ADIPOQ, LPL, PPAR and FABP4. The 2mg/ml hydrogel showed increased cytoplasmic YAP phosphorylation and reduced nuclear YAP expression compared to the 0.5mg/ml and 1mg/ml hydrogels, suggesting that stiffer ECM retains YAP in the cytoplasm, thereby enhancing adipogenesis.

Several literature references point out that in the process of mechanotransduction, YAP activity has been considered a key factor, as its nucleocytoplasmic shuttling depends on ECM stiffness [20,41]. These findings indicate that inhibiting YAP signaling significantly increases lipid droplet formation, supporting the hypothesis of a positive correlation between YAP inhibition and adipogenic differentiation.Stiffer hydrogels promote YAP phosphorylation, forcing it to remain cytoplasmic, which in turn reduces its inhibition of gene transcription and thereby enhances adipocyte differentiation. This is in agreement with the mechanosensitive properties of YAP previously reported on 2D substrates [42–44], and suggests that YAP remains a central regulator of both mechanosensing and differentiation on 3D substrates as well [25,45–47].

Although this paper has illustrated a mechanism of how the ECM stiffness may influence adipogenic differentiation, there are several limitations that have to be considered.Although our

 doi:10.20944/preprints202410.0446.v1

hydrogel model effectively simulates various ECM stiffness levels found in the adipose tissue microenvironment, it does not capture the complete complexity of the in vivo microenvironment, such as the effects of other cytokines and biochemical signals.The YAP signaling pathway is a primary focus in regulating adipogenic differentiation, whereas the roles of other mechanotransduction pathways, such as TGF-β and Wnt/β-catenin, remain poorly characterized.

Future research could further investigate how ECM composition, stiffness, and other signaling molecules interact under different physiological conditions to influence adipogenesis. Additionally, exploring methods to precisely regulate adipose tissue formation and differentiation by modulating ECM's physical properties and the YAP signaling pathway may provide novel strategies for tissue engineering and the treatment of obesity-related diseases.

5. Conclusion

This study systematically examines how extracellular matrix stiffness affects ADSC differentiation, with a focus on the YAP signaling pathway. Using different concentrations of collagen hydrogels, which allow for a good imitation of the in vivo microenvironment, we determined that the degree of adipocyte differentiation positively correlated with increased stiffness of the hydrogels. Moreover, inhibition of YAP signaling supported the accumulation of Lipid droplets (LDs), furthering the notion that ECM stiffness modulates adipogenesis by alteration of YAP's mechanosensitive properties and its phosphorylation state. Noticeably, in 2mg/mL hydrogels, larger pores and higher elastic modulus strongly supported the differentiation of ASCs. These findings unveil the regulatory role of YAP in stiffness-dependent adipogenesis, offering a novel theoretical foundation for designing tissue engineering materials and informing therapeutic strategies for obesity-related diseases.

Institutional Review Board Statement: Animal experiments received approval from the Dankook University Institutional Animal Care and Use Committee.

Acknowledgments: This work was supported by the National Research Foundation of Korea (RS-2023-00220408).

Data availability statement: The datasets generated and analyzed during this study are available from the corresponding author upon reasonable request.

Statistical Analysis: Statistical analyses were conducted using GraphPad Prism8. Differences in collagen gel contraction were analyzed using one-way ANOVA and multiple comparisons or unpaired t-tests where applicable. Western blots and BODIPY staining images were quantitatively analyzed using ImageJ-win64 software.

References

1. Diez, J.F.F.; Tegeler, A.P.; Flesher, C.G.; Michelotti, T.C.; Ford, H.; Hoque, M.N.; Bhattarai, B.; Benitez, O.J.; Christopher, G.F.; Strieder-Barboza, C. Extracellular Matrix Modulates Depot-Specific Adipogenic Capacity in Adipose Tissue of Dairy Cattle. *Journal of Dairy Science* **2024**, *0*, doi:10.3168/jds.2024-25040.
2. Karanfil, A.S.; Louis, F.; Sowa, Y.; Matsusaki, M. ECM Proteins and Cationic Polymers Coating Promote Dedifferentiation of Patient-Derived Mature Adipocytes to Stem Cells. *Biomater. Sci.* **2023**, *11*, 7623–7638, doi:10.1039/D3BM00934C.
3. Qian, Y.; Chen, H.; Pan, T.; Li, T.; Zhang, Z.; Lv, X.; Wang, J.; Ji, Z.; He, Y.; Li, L.; et al. Autologous Decellularized Extracellular Matrix Promotes Adipogenic Differentiation of Adipose Derived Stem Cells in Low Serum Culture System by Regulating the ERK1/2-PPARγ Pathway. *Adipocyte* **2021**, *10*, 174–188, doi:10.1080/21623945.2021.1906509.
4. J, C.; Y, P.; Y, L.; X, F.; T, M.; X, C.; Y, W.; X, F.; C, Z.; C, S. The Function and Mechanism of Long Noncoding RNAs in Adipogenic Differentiation. *Genes* **2024**, *15*, doi:10.3390/genes15070875.
5. Discher, D.E.; Janmey, P.; Wang, Y.-L. Tissue Cells Feel and Respond to the Stiffness of Their Substrate. *Science* **2005**, *310*, 1139–1143, doi:10.1126/science.1116995.
6. Vogel, V.; Sheetz, M. Local Force and Geometry Sensing Regulate Cell Functions. *Nat Rev Mol Cell Biol* **2006**, *7*, 265–275, doi:10.1038/nrm1890.
7. Wozniak, M.A.; Chen, C.S. Mechanotransduction in Development: A Growing Role for Contractility. *Nat Rev Mol Cell Biol* **2009**, *10*, 34–43, doi:10.1038/nrm2592.

8. DuFort, C.C.; Paszek, M.J.; Weaver, V.M. Balancing Forces: Architectural Control of Mechanotransduction. *Nat Rev Mol Cell Biol* **2011**, *12*, 308–319, doi:10.1038/nrm3112.
9. Kechagia, J.Z.; Ivaska, J.; Roca-Cusachs, P. Integrins as Biomechanical Sensors of the Microenvironment. *Nat Rev Mol Cell Biol* **2019**, *20*, 457–473, doi:10.1038/s41580-019-0134-2.
10. Baker, B.M.; Chen, C.S. Deconstructing the Third Dimension—How 3D Culture Microenvironments Alter Cellular Cues. *J Cell Sci* **2012**, *125*, 3015–3024, doi:10.1242/jcs.079509.
11. Cukierman, E.; Pankov, R.; Stevens, D.R.; Yamada, K.M. Taking Cell-Matrix Adhesions to the Third Dimension. *Developmental Dynamics* **2001**, *294*, 1708–1712, doi:10.1126/science.1064829.
12. von der Mark, K.; Gauss, V.; von der Mark, H.; Müller, P. Relationship between Cell Shape and Type of Collagen Synthesised as Chondrocytes Lose Their Cartilage Phenotype in Culture. *Nature* **1977**, *267*, 531–532, doi:10.1038/267531a0.
13. Swamydas, M.; Eddy, J.M.; Burg, K.J.L.; Dréau, D. Matrix Compositions and the Development of Breast Acini and Ducts in 3D Cultures. In Vitro *Cell Dev Biol Anim* **2010**, *46*, 673–684, doi:10.1007/s11626-010-9323-1.
14. Gerecht, S.; Burdick, J.A.; Ferreira, L.S.; Townsend, S.A.; Langer, R.; Vunjak-Novakovic, G. Hyaluronic Acid Hydrogel for Controlled Self-Renewal and Differentiation of Human Embryonic Stem Cells. *Proc Natl Acad Sci U S A* **2007**, *104*, 11298–11303, doi:10.1073/pnas.0703723104.
15. Fischbach, C.; Kong, H.J.; Hsiong, S.X.; Evangelista, M.B.; Yuen, W.; Mooney, D.J. Cancer Cell Angiogenic Capability Is Regulated by 3D Culture and Integrin Engagement. *Proc Natl Acad Sci U S A* **2009**, *106*, 399–404, doi:10.1073/pnas.0808932106.
16. Hilai, K.; Grubich, D.; Akrawi, M.; Zhu, H.; Zaghloul, R.; Shi, C.; Do, M.; Zhu, D.; Zhang, J. Mechanical Evolution of Metastatic Cancer Cells in Three-Dimensional Microenvironment. *bioRxiv* **2024**, 2024.06.27.601015, doi:10.1101/2024.06.27.601015.
17. Bono, N.; Pezzoli, D.; Levesque, L.; Loy, C.; Candiani, G.; Fiore, G.B.; Mantovani, D. Unraveling the Role of Mechanical Stimulation on Smooth Muscle Cells: A Comparative Study between 2D and 3D Models. *Biotechnol Bioeng* **2016**, *113*, 2254–2263, doi:10.1002/bit.25979.
18. Huang, W.Y.C.; Boxer, S.G.; Ferrell, J.E. Signaling Reactions in 2D vs. 3D. *Biophysical Journal* **2024**, *123*, 21a, doi:10.1016/j.bpj.2023.11.236.
19. Warren, K.M.; Islam, Md.M.; LeDuc, P.R.; Steward, R.Jr. 2D and 3D Mechanobiology in Human and Nonhuman Systems. *ACS Appl. Mater. Interfaces* **2016**, *8*, 21869–21882, doi:10.1021/acsami.5b12064.
20. Emon, B.; Joy, M.S.H.; Lalonde, L.; Ghrayeb, A.; Doha, U.; Ladehoff, L.; Brockstein, R.; Saengow, C.; Ewoldt, R.H.; Saif, M.T.A. Nuclear Deformation Regulates YAP Dynamics in Cancer Associated Fibroblasts. *Acta Biomaterialia* **2024**, *173*, 93–108, doi:10.1016/j.actbio.2023.11.015.
21. Nattasit, P.; Niibe, K.; Yamada, M.; Ohori-Morita, Y.; Limraksasin, P.; Tiskratok, W.; Yamamoto, M.; Egusa, H. Stiffness-Tunable Hydrogel-Sandwich Culture Modulates the YAP-Mediated Mechanoresponse in Induced-Pluripotent Stem Cell Embryoid Bodies and Augments Cardiomyocyte Differentiation. *Macromol Biosci* **2023**, *23*, e2300021, doi:10.1002/mabi.202300021.
22. Garrido, C.A.; Garske, D.S.; Amini, S.; Duda, G.N.; Schmidt-Bleek, K.; Cipitria, A. 3D Patterns in Alginate Hydrogel Degradation Spatially Guide YAP Nuclear Translocation and hMSC Osteogenic Differentiation 2024.
23. Na, J.; Yang, Z.; Shi, Q.; Li, C.; Liu, Y.; Song, Y.; Li, X.; Zheng, L.; Fan, Y. Extracellular Matrix Stiffness as an Energy Metabolism Regulator Drives Osteogenic Differentiation in Mesenchymal Stem Cells. *Bioactive Materials* **2024**, *35*, 549–563, doi:10.1016/j.bioactmat.2024.02.003.
24. Kersey, A.L.; Cheng, D.Y.; Deo, K.A.; Dubell, C.R.; Wang, T.-C.; Jaiswal, M.K.; Kim, M.H.; Murali, A.; Hargett, S.E.; Mallick, S.; et al. Stiffness Assisted Cell-Matrix Remodeling Trigger 3D Mechanotransduction Regulatory Programs. *Biomaterials* **2024**, *306*, 122473, doi:10.1016/j.biomaterials.2024.122473.
25. Damkham, N.; Issaragrisil, S.; Lorthongpanich, C. Role of YAP as a Mechanosensing Molecule in Stem Cells and Stem Cell-Derived Hematopoietic Cells. *Int J Mol Sci* **2022**, *23*, 14634, doi:10.3390/ijms232314634.
26. Di, X.; Gao, X.; Peng, L.; Ai, J.; Jin, X.; Qi, S.; Li, H.; Wang, K.; Luo, D. Cellular Mechanotransduction in Health and Diseases: From Molecular Mechanism to Therapeutic Targets. *Sig Transduct Target Ther* **2023**, *8*, 1–32, doi:10.1038/s41392-023-01501-9.
27. Elblová, P.; Lunova, M.; Dejneka, A.; Jirsa, M.; Lunov, O. Impact of Mechanical Cues on Key Cell Functions and Cell-Nanoparticle Interactions. *Discov Nano* **2024**, *19*, 106, doi:10.1186/s11671-024-04052-2.
28. Khussein, A.M.A. MECHANOTRANSDAUCTION: HOW CELLS SENSEAND REACT TO MECHANICAL STIMULATION. *Fundamental and applied research for key propriety areas of bioecology and biotechnology* **2023**, 168–182, doi:10.31483/r-106759.
29. Halder, G.; Dupont, S.; Piccolo, S. Transduction of Mechanical and Cytoskeletal Cues by YAP and TAZ. *Nat Rev Mol Cell Biol* **2012**, *13*, 591–600, doi:10.1038/nrm3416.
30. Dupont, S.; Morsut, L.; Aragona, M.; Enzo, E.; Giulitti, S.; Cordenonsi, M.; Zanconato, F.; Le Digabel, J.; Forcato, M.; Bicciato, S.; et al. Role of YAP/TAZ in Mechanotransduction. *Nature* **2011**, *474*, 179–183, doi:10.1038/nature10137.

31. Calvo, F.; Ege, N.; Grande-Garcia, A.; Hooper, S.; Jenkins, R.P.; Chaudhry, S.I.; Harrington, K.; Williamson, P.; Moeendarbary, E.; Charras, G.; et al. Mechanotransduction and YAP-Dependent Matrix Remodelling Is Required for the Generation and Maintenance of Cancer-Associated Fibroblasts. *Nat Cell Biol* **2013**, *15*, 637–646, doi:10.1038/ncb2756.
32. Engler, A.J.; Sen, S.; Sweeney, H.L.; Discher, D.E. Matrix Elasticity Directs Stem Cell Lineage Specification. *Cell* **2006**, *126*, 677–689, doi:10.1016/j.cell.2006.06.044.
33. Zhao, B.; Li, L.; Wang, L.; Wang, C.-Y.; Yu, J.; Guan, K.-L. Cell Detachment Activates the Hippo Pathway via Cytoskeleton Reorganization to Induce Anoikis. *Genes Dev* **2012**, *26*, 54–68, doi:10.1101/gad.173435.111.
34. Piccolo, S.; Dupont, S.; Cordenonsi, M. The Biology of YAP/TAZ: Hippo Signaling and Beyond. *Physiol Rev* **2014**, *94*, 1287–1312, doi:10.1152/physrev.00005.2014.
35. Lian, I.; Kim, J.; Okazawa, H.; Zhao, J.; Zhao, B.; Yu, J.; Chinnaiyan, A.; Israel, M.A.; Goldstein, L.S.B.; Abujarour, R.; et al. The Role of YAP Transcription Coactivator in Regulating Stem Cell Self-Renewal and Differentiation. *Genes Dev* **2010**, *24*, 1106–1118, doi:10.1101/gad.1903310.
36. Song, Y.; Na, H.; Lee, S.E.; Kim, Y.M.; Moon, J.; Nam, T.W.; Ji, Y.; Jin, Y.; Park, J.H.; Cho, S.C.; et al. Dysfunctional Adipocytes Promote Tumor Progression through YAP/TAZ-Dependent Cancer-Associated Adipocyte Transformation. *Nat Commun* **2024**, *15*, 4052, doi:10.1038/s41467-024-48179-3.
37. Quan, Y.; Shan, X.; Hu, M.; Jin, P.; Ma, J.; Fan, J.; Yang, J.; Zhang, H.; Fan, X.; Gong, Y.; et al. YAP Inhibition Promotes Endothelial Cell Differentiation from Pluripotent Stem Cell through EC Master Transcription Factor FLI1. *Journal of Molecular and Cellular Cardiology* **2022**, *163*, 81–96, doi:10.1016/j.yjmcc.2021.10.004.
38. Berthold, R.; Isfort, I.; Erkut, C.; Heinst, L.; Grünewald, I.; Wardelmann, E.; Kindler, T.; Åman, P.; Grünewald, T.G.P.; Cidre-Aranaz, F.; et al. Fusion Protein-Driven IGF-IR/PI3K/AKT Signals Deregulate Hippo Pathway Promoting Oncogenic Cooperation of YAP1 and FUS-DDIT3 in Myxoid Liposarcoma. *Oncogenesis* **2022**, *11*, 20, doi:10.1038/s41389-022-00394-7.
39. Duan, Y.; Li, X.; Zuo, X.; Shen, T.; Yu, S.; Deng, L.; Gao, C. Migration of Endothelial Cells and Mesenchymal Stem Cells into Hyaluronic Acid Hydrogels with Different Moduli under Induction of Pro-Inflammatory Macrophages. *J Mater Chem B* **2019**, *7*, 5478–5489, doi:10.1039/c9tb01126a.
40. Cai, G.; Li, X.; Lin, S.-S.; Chen, S.J.; Rodgers, N.C.; Koning, K.M.; Bi, D.; Liu, A.P. Matrix Confinement Modulates 3D Spheroid Sorting and Burst-like Collective Migration. *Acta Biomaterialia* **2024**, *179*, 192–206, doi:10.1016/j.actbio.2024.03.007.
41. Ehrlicher, A. Nuclear Mechanics and Deformation Regulate Cellular Lineage and Senescence via YAP Mechanotransduction. *Biophysical Journal* **2024**, *123*, 2a, doi:10.1016/j.bpj.2023.11.145.
42. Scott, K.E.; Fraley, S.I.; Rangamani, P. A Spatial Model of YAP/TAZ Signaling Reveals How Stiffness, Dimensionality, and Shape Contribute to Emergent Outcomes. *Proc Natl Acad Sci U S A* **2021**, *118*, e2021571118, doi:10.1073/pnas.2021571118.
43. Brusatin, G.; Panciera, T.; Gandin, A.; Citron, A.; Piccolo, S. Biomaterials and Engineered Microenvironments to Control YAP/TAZ-Dependent Cell Behavior. *Nat Mater* **2018**, *17*, 1063–1075, doi:10.1038/s41563-018-0180-8.
44. Sun, M.; Spill, F.; Zaman, M.H. A Computational Model of YAP/TAZ Mechanosensing. *Biophys J* **2016**, *110*, 2540–2550, doi:10.1016/j.bpj.2016.04.040.
45. Mikos, A.G. 3D Micropattern Force Regulates Stem Cell Function. *National Science Review* **2023**, *10*, nwad198, doi:10.1093/nsr/nwad198.
46. Virdi, J.K.; Pethe, P. Biomaterials Regulate Mechanosensors YAP/TAZ in Stem Cell Growth and Differentiation. *Tissue Eng Regen Med* **2021**, *18*, 199–215, doi:10.1007/s13770-020-00301-4.
47. Dasgupta, I.; McCollum, D. Control of Cellular Responses to Mechanical Cues through YAP/TAZ Regulation. *J Biol Chem* **2019**, *294*, 17693–17706, doi:10.1074/jbc.REV119.007963.
48. Petersen, O.W.; Rønnov-Jessen, L.; Howlett, A.R.; Bissell, M.J. Interaction with Basement Membrane Serves to Rapidly Distinguish Growth and Differentiation Pattern of Normal and Malignant Human Breast Epithelial Cells. *Proc Natl Acad Sci U S A* **1992**, *89*, 9064–9068.